Modelling analysis of centroid curves of olfactory habituation in humans

Eric Laffon, Thomas Hummel, Roger Marthan, Charlotte Sinding

Modelling analysis of centroid curves of olfactory habituation in humans

Eric Laffon [1, 2, 3] *, Thomas Hummel [4], R. Marthan [1, 2, 3], Charlotte Sinding [5]

[1] CHU de Bordeaux, Departments of Nuclear Medicine & Lung Function Testing, Bordeaux, France.

[2] Univ. Bordeaux, Centre de Recherche Cardio-Thoracique, INSERM U-1045, Bordeaux France.

[3] Inserm, Centre de Recherche Cardio-Thoracique, INSERM U-1045, Bordeaux France.

[4] Interdisciplinary Center on Smell & Taste, Department of Otorhinolaryngology, TU Dresden, Dresden, Germany.

[5] Centre des Sciences du Goût et de l'Alimentation, CNRS, UMR 6265, INRA, UMR 1324, Université de Bourgogne, Dijon, France.

*Corresponding authors:

Dr Eric Laffon, Service de Médecine Nucléaire, Hôpital du Haut-Lévêque,

Avenue de Magellan, 33604 PESSAC, France.

Telephone number: +33 5 57 65 68 38.

Fax number: +33 5 57 65 68 39.

E-mail address: elaffon@u-bordeaux.fr

Highlights

- Olfactory habituation (OH) can be considered an unconscious signal filtering
- Three centroid curves reflecting high–middle–low OH have been previously published
- Adjusting parameters of a general derived equation allowed us to fit each curve
- High correlation coefficients of 0.9997–0.9995–0.9962 were found

ABSTRACT

Previously published experiments established the time-course of olfactory habituation in humans, and extracted 3 centroid curves from clustering analysis that reflected high, middle and low habituation. The aim of the current theoretical study was to further analyze these previous experimental data by developing a mathematical modelling analysis designed for fitting the 3 curves from a general equation. After adjusting equation parameters for each curve, fitting equation outcomes on experimental data yielded high correlation coefficients of 0.9997 – 0.9995 – 0.9962, respectively. A model-based interpretation of olfactory-habituation centroid curves is proposed suggesting that they result from the effect of 2 separate processes that act simultaneously. We suggest that the first process is unlikely related to the olfactory habituation itself, and, rather, is of unclear origin. The second process seems to play a major role in the degree of OH and cannot be assigned, a priori, to either peripheral or central adaptation, respectively.

1. Introduction

Olfactory habituation (OH) can be considered an unconscious filter whose role is to avoid brain overstimulation [1-5]. New determinants of OH have been reported in humans by Sinding et al., showing that reduced responsiveness to a continuous or repetitive stimulation depends on some properties of the odorant, notably trigeminality and associated physicochemical characteristics [6]. In these previous experiments, the course of odor intensity of 32 different odorants, which differed in physicochemical characteristics and were presented at constant flow during 120s, was rated continuously by 58 participants. A k-means clustering analysis of the 1856 recorded curves allowed the authors to partition the data into 3 clusters, thus providing 3 normalized centroid curves representing high, middle and low habituation (HH, MH, LH), respectively. The current study focuses on the HH – MH – LH experimental data that were re-analyzed by means of a mathematical modelling analysis in order to provide further model-based information about the processes and mechanisms underlying OH centroid curves in humans.

In line with Sinding et al. [6], we used, in the current study, the term habituation for the perceptual decrement of odor intensity [4,7], and adaptation when addressing the underlying mechanisms. The term peripheral adaptation encompasses all the adaptation mechanisms that may occur at the receptor level, and the term central adaptation encompasses all the adaptation mechanisms that tune the olfactory signal coming up from the olfactory neurons [7]. Likewise, in this study, 2 adaptation mechanisms were considered, namely, intensity-limiting and intensity-decreasing mechanisms, which were not assigned to either peripheral or central adaptation, respectively. More specifically, the term of intensity-limiting mechanism referred to the situation where the odor intensity (i.e., the signal) under constant odorant-concentration conditions cannot increase with time above a certain value. The term of intensity-decreasing mechanism referred to the situation where the odor intensity (i.e., the

signal) decreases with time even if the odorant concentration is constant. Noteworthy, this definition only considered a time-dependency of the two mechanisms and investigating the role of a dose-dependency was out of the scope of the current study, as well as of the previous one [6].

Although the comparison of HH – MH – LH centroid curves emphasized the differential filtering of the olfactory signal, depending on the odorant, we nevertheless suggest that the 3 different centroid curves share a common set of processes, each involving intensity-limiting and intensity-decreasing mechanisms, without assigning, a priori, any process or any mechanism to either peripheral or central adaptation. Therefore, the aim of the current study was to derive a general equation of the OH centroid curves from a mathematical modelling analysis, involving intensity-limiting and intensity-decreasing parameters whose value can be adjusted to fit each experimental OH centroid curve.

2. Material and methods

2.1 Mathematical modelling analysis

We assume that the rate of change in the OH signal, i.e., dS(t)/dt, can be written as:

$$dS(t)/dt = L(t) \times N_0 - k_{dec} \times S(t) \tag{1}$$

where (i) L(t) represents an intensity-limiting time function, (ii) k_{dec} represents an intensity-decreasing time constant (in s^{-1}) and (iii) N_0 is the odorant molecule amount in the nasal cavity that is constant with time since the OH experiments were performed under continuous delivery of odorant at constant concentration [6]. Let us further assume that L(t) can be expressed by means of a sum of exponentially time-decreasing functions ($L_i(t)$; amplitude: L_i, in arbitrary unit; time constant: k_{Li}, in s^{-1}):

$$L(t) = \sum L_i(t) = \sum L_i \times \exp(- k_{Li} \times t) \tag{2}$$

As a consequence, the solution of Equation (1) is a sum of separate processes, i.e., $S_i(t)$, each involving its own intensity-limiting parameters (A_i, k_{Li}), but all having the same intensity-decreasing time constant (k_{dec}):

$$S(t) = \sum S_i(t) = \sum S_i \times [\exp(-k_{Li} \times t) - \exp(- k_{dec} \times t)] / [k_{dec} - k_{Li}] \tag{3}$$

where $S_i = N_0 \times L_i$ (in arbitrary unit: a.u.).

2.1 Fitting of OH centroid curves

We preliminarily verified the Equation-(1) assumption of the 1 intensity-decreasing time constant (k_{dec}) by fitting the last part of the HH curve with a mono-exponentially decreasing function (GraphPad Prism software, version 5.00).

Then, since intensity ratings previously reported by Sinding et al. always started at level 6 (by using a device that transformed pressure into a signal ranging between 0 and 10), the fitting of each experimental OH curve was performed by using nonlinear regression (GraphPad Prism software, version 5.00) from this level and over the entire stimulation period

of 120 s. Different fittings of Equation (3) on HH – MH – LH experimental data were performed assuming L(t) involves 1 or a sum of several intensity-limiting functions, in other words, assuming S(t) involves 1 or a sum of several processes.

2.3 Statistical analysis

The fittings allowed us to assess parameters involved in Equation (3), i.e., S_i, k_{Li} and k_{dec} for each HH – MH – LH curve, respectively, along with their standard deviation (SD). In the framework of a two-process OH signal, i.e., involving the 5 parameters $S_{1,2}$, $k_{L1,2}$ and k_{dec}, standard deviation of the ratio S_1/S_2 was computed from the following equation for each HH – MH – LH curve:

$$(SD_{S1/S2})^2 = (S_1/S_2)^2 [(SD_{S1}/S_1)^2 + (SD_{S2}/S_2)^2] \tag{4}$$

A weighted mean value of k_{L1} was obtained from the 3 values and their SD assessed from the 3 HH – MH – LH curves, as:

$$< k_{L1}> = SD_{kL1}{}^2 [k_{L1-HH}/(SD_{kL1-HH})^2 + k_{L1-MH}/(SD_{kL1-MH})^2 + k_{L1-LH}/(SD_{kL1-LH})^2] \tag{5}$$

with $SD_{kL1}{}^2$ computed from the equation:

$$SD_{kL1}{}^2 = [(1/SD_{kL1-HH})^2 + (1/SD_{kL1-MH})^2 + (1/SD_{kL1-LH})^2]^{-1} \tag{6}$$

For all statistical tests, a P-value below 0.05 was considered to be statistically significant. Confidence intervals of the parameter estimates were calculated as 1.96×SD, with 95% reliability.

3. Results

The preliminary fitting of the last part of the HH curve with a mono-exponentially decreasing function, yielded a correlation coefficient of $R = 0.9989$ (range 50 – 120 s; graph not shown), thus allowing us the fitting of Equation (3) on HH – MH – LH experimental data. The highest correlation coefficient of Equation-(3) fitting on HH – MH – LH experimental data was obtained when S(t) involves two processes: $R = 0.9997 – 0.9995 – 0.9962$ for the graph displaying HH – MH – LH experimental versus theoretical data (Figure 1a,b,c; n = 465 – 466 – 465; $P < 0.001$), respectively (graphs of one-process HH – MH – LH not shown). We therefore did not further probe a three-process fitting, and S(t) can be expressed as:

$$S(t) = S_1(t) + S_2(t)$$

$$= S_1 \times [\exp(- k_{L1} \times t) - \exp(-k_{dec} \times t)] / [k_{dec} – k_{L1}]$$

$$+ S_2 \times [\exp(- k_{L2} \times t) - \exp(-k_{dec} \times t)] / [k_{dec} – k_{L2}] \qquad (7)$$

Figure 2 illustrates the respective part of intensity-limiting and intensity-decreasing mechanisms in the HH signal. Table 1 summarizes the fitting outcomes of the 5 parameters, i.e., $S_{1,2}$, $k_{L1,2}$ and k_{dec}, for HH – MH – LH. Confidence intervals (CI; with 95% reliability) calculated from SD in Table 1 indicate that S_2 and k_{L2} were significantly different between HH, MH and LH, respectively. Moreover, the ratio S_1/S_2 was significantly different between HH, MH and LH: 6.62 ± 0.39, 11.57 ± 1.00 and 18.07 ± 2.48 ($\pm$ 95% CI), respectively. A weighted mean k_{L1} value was computed from HH – MH – LH data: $\langle k_{L1} \rangle = 0.35710 \pm 0.00451$ s^{-1}, that is, with $\pm$ 1.3% relative measurement uncertainty (95% reliability). Figure 3a, b, c separately shows $S_1(t)$ and $S_2(t)$ expressed in the right hand side of Equation (7). In other words, the sum "$S_1(t) + S_2(t)$" of the curves shown in Figure 3a, 3b and 3c is the curve shown in Figure 1a, 1b and 1c for HH – MH – LH, respectively. Figure 4 shows the comparison between $S_1(t)$ of HH and $S_1(t)$ of both MH and LH, after arbitrarily setting the k_{dec} value of the latter to that of the former (Table 1).

4. **Discussion**

Sinding et al. previously showed that the unconscious filter of OH, which is designed to avoid brain overstimulation, depends on the odorant [6]. The authors illustrated this finding with 3 normalized centroid curves of different shapes, characterizing High Habituation, Medium Habituation and Low Habituation. These OH curves were obtained under constant olfactory stimulation, but all exhibited a similar pattern consisting in a peak followed by a decrease. Actually, this pattern can be interpreted as a combination of intensity-limiting and intensity-decreasing mechanisms, as illustrated in Figure 2 for HH. An intensity-limiting mechanism alone would lead the OH signal to reaching a plateau, even under conditions of a constant stimulation with an odorant, that differs from that of the maximum intensity perceived reported in literature [8]. The intensity-decreasing mechanism, which is effective simultaneously with the former, modifies this plateau by inducing a decrease. As a result, combining intensity-limiting and intensity-decreasing mechanisms generates a peak then followed by a decrease. Therefore, the current study aimed at deriving a general equation from a mathematical modelling analysis involving these 2 mechanisms (Equations (2-3-7)). Adjusting 4 intensity-limiting and 1 intensity-decreasing parameters of this general equation enabled us to fit each HH – MH – LH centroid curves, respectively. The finding of 1 intensity-decreasing time constant, i.e. k_{dec}, for each HH – MH – LH curve, respectively, confirmed the preliminary fitting of the last part of the HH curve with a mono-exponentially decreasing function and, thereby, confirmed the Equation-(1) assumption of the 1 intensity-decreasing time constant. Correlation coefficients of experimental versus theoretical (Equation (7)) data fitting were high: $R = 0.9997 – 0.9995 – 0.9962$ ($P < 0.001$) for HH – MH – LH (Figure 1), respectively. Moreover, for each quantitative parameter and for each OH degree, the SD was small in comparison with its estimate (Table 1). Hence, we believe that

these features support the relevance of the proposed mathematical modelling analysis of the OH centroid curves in humans.

Equation (7) shows that the OH centroid curves result from the sum of 2 processes, i.e., "$S_1(t) + S_2(t)$", that are related to 2 intensity-limiting functions, i.e., $L_1(t)$ and $L_2(t)$ (Equation (2)), that exponentially decrease with a different time constant (Table 1). Comparison of $S_1(t)$ and $S_2(t)$ between HH, MH and LH in Figure 3 apparently indicates that both are different in relation to the degree of OH. However, after arbitrarily setting the k_{dec} value in both MH and LH to that of HH (Table 1: $k_{dec} = 0.02286$ s^{-1}), "corrected" $S_1(t)$ of MH and LH then appears to be close to that of HH, within 95%-CI limit of HH in Figure 4. This finding is consistent with the comparison of S_1 and k_{L1} values found for HH, MH and LH in Table 1. Thus, the difference occurring in the decreasing part of $S_1(t)$ between HH, MH and LH (Figure 3) is related to the value of the intensity-decreasing time constant that diminishes from HH to LH: the lower the k_{dec} value, the shallower the decreasing part of $S_1(t)$ and, in terms of OH, the more prolonged the perception of odorant intensity. We therefore suggest that, whatever the OH degree, a first, shared, intensity-limiting mechanism occurs that is, nevertheless, tuned by the specific intensity-decreasing time constant of the OH degree. In contrast, S_2 and k_{L2} values were significantly different between HH, MH and LH, respectively, ruling out such a sharing feature for $S_2(t)$ (Table 1). Furthermore, whereas $S_2(t)$ reinforces the $S_1(t)$ process in HH (Figure 3a), it plays a distinct role from $S_1(t)$ in LH (Figure 3c). Indeed, the lower the OH degree, the lower the S_2 and k_{L2} value (Table 1) and the weaker the role of the second process, thus allowing prolonged perception of odor intensity, although at a low level. This prolonged perception in LH is strengthened by a low value of the intensity-decreasing time constant, in line with what has been above commented for $S_1(t)$.

An interpretation of the 2 processes involved in the 3 OH centroid curves, i.e., $S_1(t)$ and $S_2(t)$, may be hypothesized. Figure 3 shows that $S_1(t)$ plays a major role in the rising part

and in the peak of each OH centroid-curve. We suggest that $S_1(t)$ is very likely affected by the somewhat problematic onset ratings (even beginning at $y = 0.6$) and that, since the current modelling analysis established that S_1 and k_{L1} values were found to be shared by the whole OH centroid curves, these imperfect ratings affected in a similar manner both HH, MH and LH centroid curves. As a consequence, we suggest that the first intensity-limiting mechanism, and, hence, $S_1(t)$, may be mainly related to the experimental design involving the whole unknown signal-transmission features occurring from the olfactory epithelium to the response given by the subject, who, furthermore, started intensity ratings at level 6 by using a device that transformed pressure into a signal ranging between 0 and 10. In other words, we suggest that $S_1(t)$ is unlikely related to the olfactory habituation itself and, rather, may possibly be of artifactual origin. In contrast, we hypothesize that $S_2(t)$ plays a major role in the OH degree, since S_2 and k_{L2} values were found to be significantly different between HH, MH and LH, respectively. However, its origin is not clear and, at this stage of our work, $S_2(t)$ cannot be specifically assigned to either peripheral or central adaptation, respectively. Due to the limited knowledge on the central processes involved in adaptation [7], we can assume that both central and peripheral adaptation very likely occur in combination for achieving OH during a 2-minute continuous odorant-stimulation condition. Finally, it should be noted that the mathematical expression of $S_1(t)$ and $S_2(t)$ is similar to that of the conductance change due to a presynaptic event [9], which thereby involves conductance-limiting and conductance-decreasing mechanisms.

The interpretation of the mathematical model analysis is limited regarding the amplitudes of $S_1(t)$ and $S_2(t)$, that is, about S_1 and S_2 in Equation (7). This is because the HH – MH – LH curves were previously normalized before being fitted. Therefore, the amplitude comparison was limited to the S_1/S_2 ratio that was significantly different between HH, MH and LH, respectively (95% reliability). This, nevertheless, remains of limited interest in

contrast to comparing absolute values of the corresponding time constants k_{L1} and k_{L2} (Figure 3; Table 1). It is worth noting that $S_{1,2}$ were expressed as $S_{1,2} = L_{1,2} \times N_0$, and then if the S_1/S_2 ratio is known, the L_1/L_2 ratio is known too. Actually, $L_{1,2}$ involves (i) the total number of different receptors recruited by an arbitrary odorant molecule that might depend on the process and on N_0 [8], respectively, and (ii) the whole unknown signal-transmission features occurring from the olfactory epithelium to the intensity ratings that might depend on the process.

Since the current modelling analysis allowed us to distinguish between $S_1(t)$ and $S_2(t)$, and that $S_2(t)$ may play a major role in the OH degree, we suggest that a future goal could be to implement the current modelling analysis in OH centroid curves obtained for different odorants, focusing on $S_2(t)$, that is, on S_2, k_{L2} and k_{dec} . In such a framework, curve fitting might be simplified in comparison with the current one by assessing 4 parameters (i.e., $S_{1,2}$, k_{L2} and k_{dec}), instead of 5 parameters, since the current results allow us to assume that k_{L1} is identical for any odorant. Determinants of OH that have been previously reported could be re-examined, as well as combinations of factors [6]. Furthermore, a dose-dependency of the intensity-limiting and intensity-decreasing mechanisms, and, hence, of $S_1(t)$ and $S_2(t)$, could be investigated. Dose-dependent changes in the parameter values of the mechanisms may indeed be expected. The efficiency of the clustering analysis, and, hence, the accuracy of the proposed mathematical modelling analysis, will require a great amount of data for such investigations in order to get rid of random and unwanted factors, including technical and emotional factors [10].

To conclude, for the first time, to the best of our knowledge, a mathematical modelling analysis is proposed enabling us to fit different degrees of human OH corresponding to 3 centroid curves extracted from a clustering analysis [6]. By simply adjusting 5 parameters involved in the same general equation, fitting correlation coefficients of HH – MH – LH

curves were high: 0.9997 – 0.9995 – 0.9962, respectively. The general equation suggests that each OH centroid curve results from the simultaneous effect of 2 separate processes, i.e. $S_1(t)$ and $S_2(t)$, each involving its own intensity-limiting mechanism but having the same intensity-decreasing mechanism, respectively. The first process, i.e. $S_1(t)$, is of unclear, possibly artifactual origin, and, thereby, is unlikely related to the olfactory habituation itself. In contrast, we suggest that the second process, i.e. $S_2(t)$, which appeared to depend on the odorant, plays a major role in the OH degree and cannot be assigned, a priori, to either peripheral or central adaptation, respectively. The proposed mathematical modelling analysis emphasizes that relevant olfactory research data can be obtained in a non-invasive manner, putting forward the usefulness of the clustering-analysis tool.

Author Contributions

Mathematical modelling analysis: E.L.; interpretation of the mathematical modelling analysis: E.L., C.S; design of the study, discussion, writing and reviewing of the manuscript: E.L., T.H., R.M., C.S.

## Competing interests

The authors declare no competing interests.

References

1. R. F. Thompson, W.A. Spencer, Habituation: a model phenomenon for the study of neuronal substrates of behaviour, Psychol. Rev. 73 (1966) 16–43.

2. D.A. Wilson, Habituation of odor responses in the rat anterior piriform cortex, J. Neurophysiol. 79 (1998) 1425–1440.

3. A. Poellinger, Activation and habituation in olfaction—an fMRI study, Neuroimage. 13 (2001) 547–560.

4. R.F. Thompson, Habituation: a history. Neurobiol. Learn. Mem. 92 (2009) 127–134.

5. C.H. Rankin, Habituation revisited: an updated and revised description of the behavioral characteristics of habituation, Neurobiol. Learn. Mem. 92 (2009) 135–138.

6. C. Sinding, F. Valadier, V. Al-Hassani, G. Feron, A. Tromelin, I. Kontaris, T. Hummel, New determinants of olfactory habituation. Sci. Rep. 7 (2017) 41047–41058.

7. R. Pellegrino, C. Sinding, R.A. de Wijk, T. Hummel, Habituation and adaptation to odors in humans. Physiol Behav. 177 (2017) 13–19.

8. M. Chastrette, T. Thomas-Danguin, E. Rallet, Modelling the human olfactory stimulus-response function. Chem Senses. 23 (1998) 181-196.

9. C. Linster, A.V. Menon, C.Y. Singh, D.A. Wilson, Odor-specific habituation arises from interaction of afferent synaptic adaptation and intrinsic synaptic potentiation in olfactory. Learn. Mem. 16 (2009) 452–459.

10. J. Lötsch, D. Kringel, T. Hummel, Machine learning in human olfactory research. Chemical Senses 44 (2019) 11–22.

Table 1. Fitting results (±SD) of intensity-versus-time OH curves, by using Equation (7).

	High Habituation	Middle Habituation	Low Habituation
S_1 (a.u.)	0.245 ±0.003	0.266 ±0.002	0.271 ±0.002
k_{L1} (s^{-1})	0.32463 ±0.00718	0.36156 ±0.00447	0.35525 ±0.00287
S_2 (a.u.)	0.037 ±0.001	0.023 ±0.001	0.015 ±0.001
k_{L2} (s^{-1})	0.05416 ±0.00201	0.03220 ±0.00099	0.01042 ±0.00007
k_{dec} (s^{-1})	0.02286 ±0.00027	0.01253 ±0.00020	0.01042 ±0.00049

a)
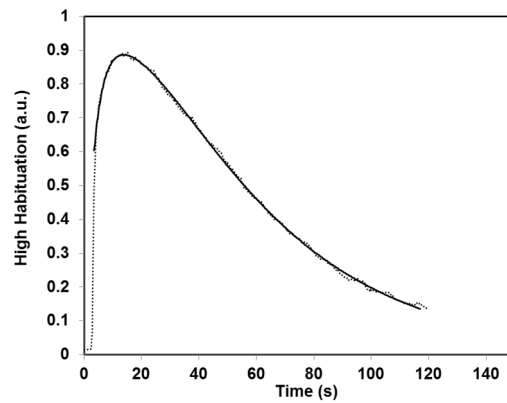
b)
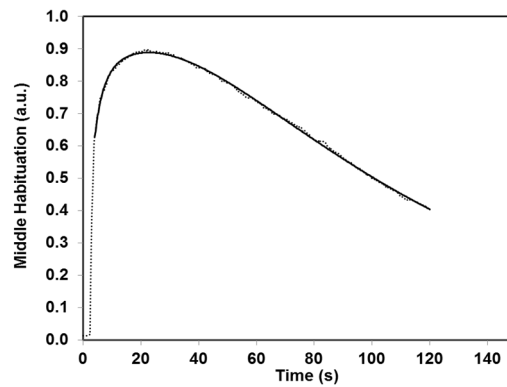
c)
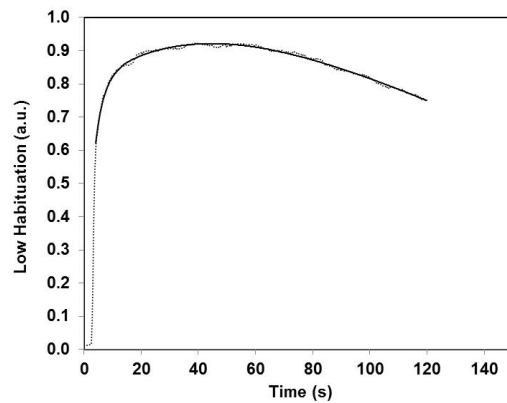
Figure 1. Fitting of intensity-versus-time OH centroid curves. Intensity in arbitrary unit (a.u.) and time in second (s). Experimental data (dotted line) and fitting outcomes of Equation (7) (full line) for a) HH ($R = 0.9997$), b) MH ($R = 0.9995$) and c) LH ($R = 0.9962$), respectively ($P < 0.001$ for all curves). All fittings started at y = 0.6 since subjects were asked to start evaluating intensity at the level 6 (range 0 to10).
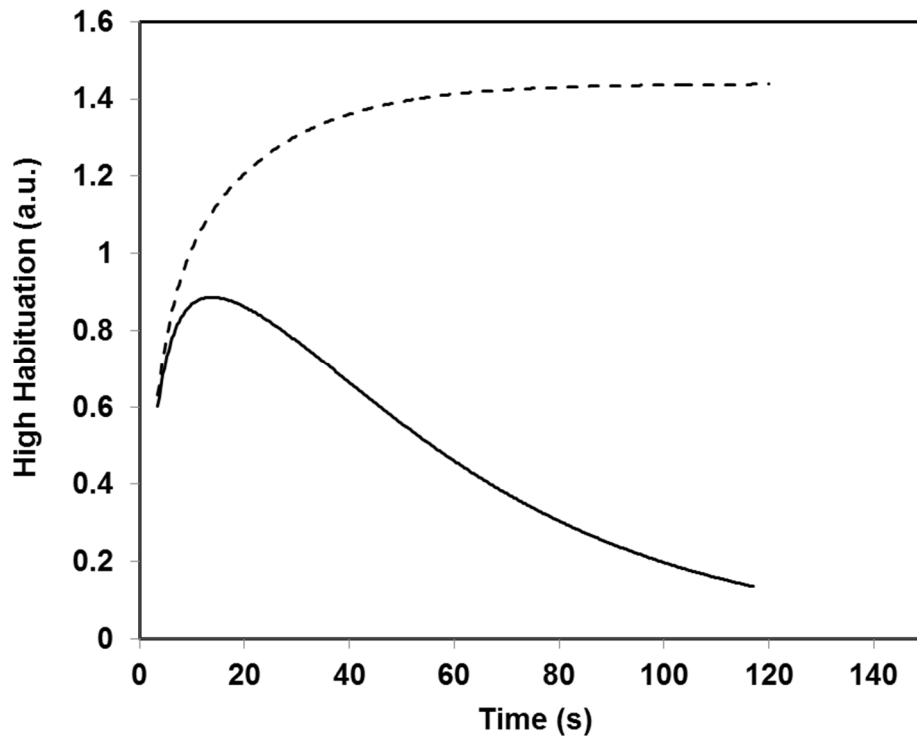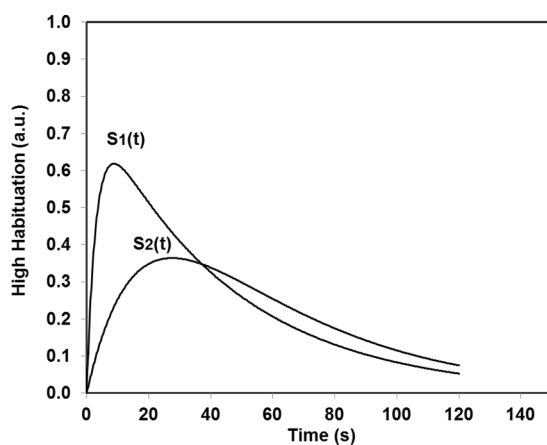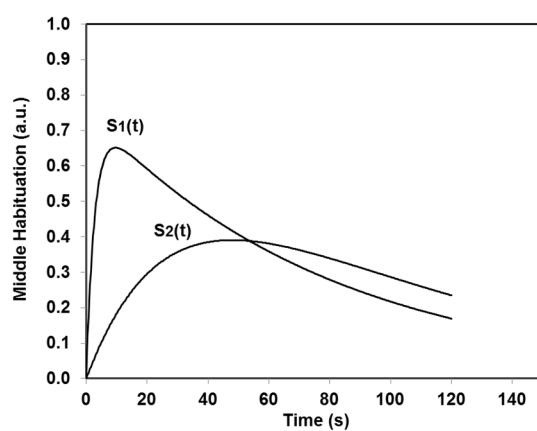
Figure 2. Intensity-limiting versus intensity-decreasing mechanisms for HH.

Fitting outcomes of Equation (7) already shown in Figure 1a (full line), versus outcomes of Equation (7) after setting k_{dec} to zero (dashed line).
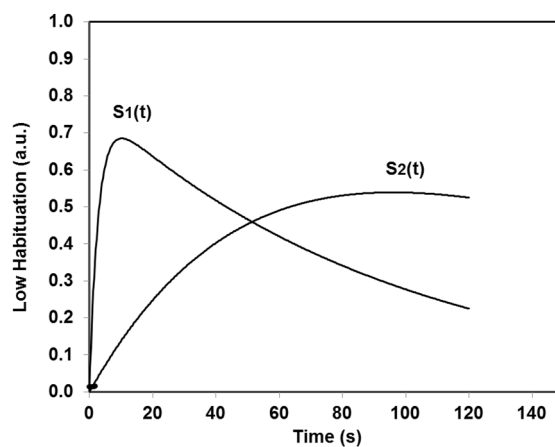
a)

b)

c)

Figure 3. Role in the whole OH centroid curves the 2 processes $S_1(t)$ and $S_2(t)$.

$S_1(t)$ and $S_2(t)$ involve the parameter estimates assessed by fitting the whole OH centroid curves (Table 1), for a) HH, b) MH and c) LH, respectively. The resulting curve of the sum "$S_1(t) + S_2(t)$" in Figure 3a, b, c is the curve shown in Figure 1a, b, c, respectively.
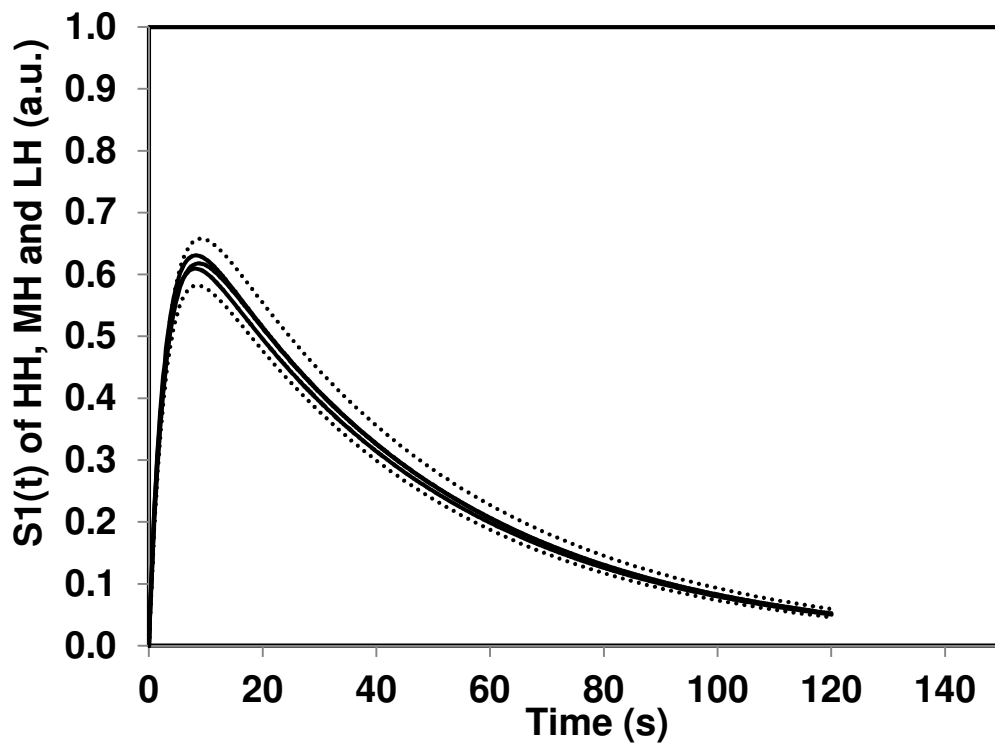
Figure 4. Comparison between $S_1(t)$ of HH, MH and LH.

$S_1(t)$ of HH, MH and LH was compared after arbitrarily setting the same k_{dec} value to both (full line); 95% CI of the HH $S_1(t)$ curve is shown (dotted lines).